Power System Time Domain Simulation Using a Differential Transformation Method

Yang Liu, *Student Member, IEEE*, Kai Sun, *Senior Member, IEEE,* Rui Yao, *Member, IEEE,* and Bin Wang, *Member, IEEE*

***Abstract*— This paper proposes a novel approach for power system dynamic simulation based on the Differential Transformation (DT). The DT is introduced to study power systems as high-dimensional nonlinear dynamical systems for the first time, and is able to avoid computations of high-order derivatives with nonlinear differential equations by its transform rules. This paper first proposes and proves several new transform rules for generic non-linear functions that often appear in power system models, and then uses these rules to transform representative power system models such as the synchronous machine model with trigonometric functions and the exciter model with exponential and square root functions. The paper also designs a DT-based simulation scheme that allows significantly prolonged time steps to reduce simulation time compared to a traditional numerical approach. The numerical stability, accuracy and time performance of the proposed new DT-based simulation approach are compared with widely used numerical methods on the IEEE 39-bus system and Polish 2383-bus system.**

***Index Terms*—Differential transformation method; power system simulation; transient stability; numerical integration.**

I. Introduction

POWER system dynamic simulation is of critical importance for utilities to assess the dynamic security by solving the initial value problem of power system nonlinear differential equations (DEs) with a given contingency occurring under a specific operating condition [1]. Numerical integration methods, including explicit and implicit methods, are commonly used in commercial software packages with a small enough integration step of typically several to tens of milliseconds to meet accuracy and numerical stability requirements [2]-[3]. In recent years, the power systems have been pushed to be operated closer to their stability limits due to the fast growth of electricity demands but a relatively slow construction of new transmission infrastructure. To identify any insecure contingency before it happens, time domain simulation is expected to be transitioned from offline or day-ahead studies to the real-time operation environment. The power industry and research community seek next-generation simulation tools which are more powerful for power system dynamic security assessment in real time [4]-[17].

One way to speed up simulation by traditional numerical integration methods is to incorporate parallel computing [4]-[11]. With the fast development of high performance computers, a variety of parallel power system simulation methods have been proposed to decompose system models or computation tasks in simulation. Paper [4] decomposes a system model into three linear subsystems and ensures simulation accuracy by adaptive updates on linear subsystems. Paper [5] proposes a two-stage parallel waveform relaxation method for parallel simulation, which adopts epsilon decomposition to partition a large-scale power system model into several subsystems. A Schur-complement based network decomposition method is proposed in [6]. The parareal in time method in [7] and [8] adopts temporal decomposition of the simulation period into many intervals, conducts parallel simulations on individual intervals using a fine solver, and connects their results by a high-level coarse solver after a few iterations. A multi-area Thevenin equivalents method is also studied in [9]. Recently, paper [10] develops a practical framework to parallelize computation tasks of a single dynamic simulation in commercial software and paper [11] designs a massively parallel computational platform for efficient dynamic security assessment. Except for numerical methods, some alternative simulation methods are also proposed in literature such as semi-analytical methods [12]-[16].

This paper proposes a novel dynamic simulation approach based on Differential Transformation (DT), which is a mathematical tool and can effectively find an approximate solution of a set of nonlinear DEs. The paper, for the first time, introduces DT to power system studies. By assuming the solution of a set of power system DEs as a power series in time, the proposed approach utilizes DT to calculate series coefficients efficiently by means of a set of transform rules designed for nonlinear functions involved in power system models instead of directly computing the high-order derivatives in DEs. These transform rules are proved for representative power system models including a detailed synchronous machine model involving trigonometric functions and a practical exciter model with the exponential and square root functions. The paper also proposed a DT-based dynamic simulation scheme that allows significantly prolonged time steps to reduce the overall simulation time compared to a traditional numerical approach.

This work was supported in part by the ERC Program of the NSF and DOE under NSF Grant EEC-1041877 and in part by the NSF Grant ECCS-1610025.

Y. Liu, K. Sun, R. Yao, B. Wang are with the Department of EECS, University of Tennessee, Knoxville, TN 37996 USA (e-mail: yliu161@vols.utk.edu, kaisun@utk.edu, ryao3@utk.edu, bwang13@vols.utk.edu).

The rest of the paper is organized as follows. Section II introduces DT and its basic transform rules. Section III proposes and proves the transform rules specifically designed for power system models. Section IV presents the proposed DT-based simulation scheme. Section V tests the numerical stability, accuracy and time performance of the proposed scheme on the 10-machine 39-bus New England system and a Polish 327-machine 2383-bus system. Finally, conclusions are drawn in section VI.

II. Introduction of the Differential Transformation

For a set of nonlinear DEs that models a dynamical system, the explicit, analytical solution does not exist in general. However, an approximate solution can be represented by a finite power series in time up to a designed order. Thus, calculating power series coefficients would be a key to obtain such an approximate solution.

The DT is an effective mathematical tool to serve this purpose. It has been studied by researchers in the fields of applied mathematics and physics for various nonlinear dynamic systems such as the Van der Pol oscillator, Duffing equations and fractional order systems [18]-[26]. In existing literature, the DT is mainly applied to small systems described by low-order DEs and its capability has not been examined for real-life complex network systems like power systems modeled by a large set of nonlinear DEs. This section introduces the definition and rules of the DT and Section III will apply the DT to power system models.

Definition: Consider a function $x(t)$ of a real continuous variable *t*. The DT of $x(t)$ is defined by (1), and the inverse DT of $X(k)$ is defined by (2), where $k \in \mathbb{N}$ is the order.

$$X(k) = \frac{1}{k!}\left[\frac{d^k x(t)}{dt^k}\right]_{t=0} \tag{1}$$

$$x(t) = \sum_{k=0}^{\infty} X(k)\, t^k \tag{2}$$

The DT method provides a set of transform rules such as those in the following Proposition 1 and Proposition 2. Their detailed proofs can be found in [18].

Proposition 1: Denote $x(t)$, $y(t)$ and $z(t)$ as the original functions and $X(k)$, $Y(k)$ and $Z(k)$ as their DTs, respectively. The following propositions (a) - (f) hold, where c is a constant, n is a nonnegative integer and ϱ is the Kronecker delta function defined in discrete domain.

(a) $X(0) = x(0)$.

(b) $y(t) = cx(t) \rightarrow Y(k) = cX(k)$.

(c) $z(t) = x(t) \pm y(t) \rightarrow Z(k) = X(k) \pm Y(k)$.

(d) $z(t) = x(t)y(t) \rightarrow Z(k) = \sum_{m=0}^{k} X(m)Y(k-m)$.

(e) $y(t) = t^n \rightarrow Y(k) = \varrho(k-n) = \begin{cases} 1, & k = n \\ 0, & k \neq n \end{cases}$.

(f) $y(t) = c \rightarrow Y(k) = c\varrho(k) = \begin{cases} c, & k = 0 \\ 0, & k \neq 0 \end{cases}$

(g) $y(t) = \frac{dx(t)}{dt} \rightarrow Y(k) = (k+1)X(k+1)$.

Proposition 2: If $\phi(t) = \sin\delta(t)$, $\psi(t) = \cos\delta(t)$ and $\Phi(k)$, $\Psi(k)$ and $\Delta(k)$ are the DTs of $\phi(t), \psi(t)$ and $\delta(t)$, respectively, then $\Phi(k)$ and $\Psi(k)$ are calculated by:

$$\begin{aligned} \Phi(k) &= \sum_{m=0}^{k-1} \frac{k-m}{k} \Psi(m)\Delta(k-m) \\ \Psi(k) &= -\sum_{m=0}^{k-1} \frac{k-m}{k} \Phi(m)\Delta(k-m) \end{aligned} \tag{3}$$

III. DTs of Power System Models

The Taylor series of a nonlinear function can more easily be obtained by using the DT with the above transform rules than directly using the traditional Taylor expansion formulas. This section presents the DTs of several representative power system models, which include the detailed 6th order synchronous machine model, the first order governor and first order turbine model, the IEEE Type I exciter model and the first order PSS (power system stabilizer) model.

A. New Transform Rules for Power System Models

The main idea of deriving the DT of a power system model is to apply DT to both sides of each equation. However, besides the nonlinear functions involved in Propositions 1 and 2, there are other commonly used nonlinear functions in power system models whose transform rules are not provided by the original DT theory, such as composite exponential functions, square root functions and fractional functions. This paper has further proved the transform rules of these functions according to the basic idea in [18] as follows. The detailed proofs are provided in the Appendix. These additional transform rules together with the basic transform rules can be implemented by a software library in a symbolic computing environment, e.g. Mathematica and Maple. Thus, the whole procedure of DT for a power system model can become automated.

Proposition 3: Given function $y_1(t) = e^{x(t)}$, if $Y_1(k)$ and $X(k)$ are the DTs of $y_1(t)$ and $x(t)$, respectively, then $Y_1(k)$ is calculated by:

$$Y_1(k) = \frac{1}{k}\sum_{m=0}^{k-1} (k-m)Y_1(m)X(k-m) \tag{4}$$

Proposition 4: Given function $y_2(t) = \sqrt{x}$, $Y_2(k)$ and $X(k)$ are the DTs of $y_2(t)$ and $x(t)$, respectively, and

$$Y_2(k) = \frac{1}{2Y_2(0)}X(k) - \frac{1}{2Y_2(0)}\sum_{m=1}^{k-1} Y_2(m)Y_2(k-m) \tag{5}$$

Proposition 5: Given function $z(t) = x(t)/y(t)$, if $X(k)$, $Y(k)$ and $Z(k)$ are the DTs of $x(t)$, $y(t)$ and $z(t)$, respectively, then $Z(k)$ is calculated by:

$$Z(k) = \frac{1}{Y(0)}X(k) - \frac{1}{Y(0)}\sum_{m=0}^{k-1} Z(m)Y(k-m) \tag{6}$$

To be differentiated from original functions, e.g. $e_{fd}(t), v_r(t)$, their DTs are denoted using capital letters, e.g., $E_{fd}(k)$ and $V_r(k), k = 0,1,2\ldots K$. Besides, time "$t$" of original functions are omitted for simplicity, i.e. $e_{fd}(t), v_r(t) \rightarrow e_{fd}, v_r$.

B. Governor Model

The equation of a 1st order governor model [13] is given in (7), where p_{sv} is the governor output power, p_{ref} is the electrical power setting point and s_m is rotor slip; T_{sv} and R_d are governor time constant and the droop coefficient.

$$T_{sv}\dot{p}_{sv} = -p_{sv} + p_{ref} - \frac{1}{R_d}s_m \tag{7}$$

The DTs of the four terms in (7) can be obtained using Proposition 1 as explained in detail in the following:

1) The LHS (left hand side) term $T_{sv}\dot{p}_{sv}$ is a product of a constant and the derivative of p_{sv}. The DT of $\dot{p}_{sv}$ can be obtained from Proposition 1-g:

$$\dot{p}_{sv} \rightarrow (k+1)P_{sv}(k+1)$$

Then the DT of $T_{sv}\dot{p}_{sv}$ can be obtained from Proposition 1-b:

$$T_{sv}\dot{p}_{sv} \rightarrow (k+1)T_{sv}P_{sv}(k+1)$$

2) Similarly, the DTs of three RHS (right hand side) terms can be obtained using Proposition 1-b:

$$-p_{sv} \rightarrow -P_{sv}(k)$$

$$p_{ref} \rightarrow p_{ref}\varrho(k)$$

$$-\frac{1}{R_d}s_m \rightarrow -\frac{1}{R_d}S_m(k)$$

Finally, the original equation becomes

$$(k+1)T_{sv}P_{sv}(k+1) = -P_{sv}(k) + p_{ref}\varrho(k) - \frac{1}{R_d}S_m(k) \tag{8}$$

C. Turbine Model

Consider the 1st order turbine model [13] given in (9) about mechanical power p_m with time constant T_{ch}:

$$T_{ch}\dot{p}_m = -p_m + p_{sv} \tag{9}$$

Similar to the above procedure for the governor model, apply DT to its both sides:

$$(k+1)T_{ch}P_m(k+1) = -P_m(k) + P_{sv}(k) \tag{10}$$

D. PSS Type I Model

A PSS Type I model [3] is given in (11), where v_s is the PSS output voltage that is used to modify the exciter reference voltage; the input signal is the rotor speed w, electrical power p_e and bus voltage magnitude v_t; T_w is the time constant and K_w is the stabilizer gain.

$$\begin{aligned} T_w\dot{v}_1 &= -\left(K_w w + K_p p_e + K_v v_t + v_1\right) \\ v_s &= K_w w + K_p p_e + K_v v_t + v_1 \end{aligned} \tag{11}$$

Similar with the procedure for governor and turbine model, the DT on the PSS model can be written in (12).

$$\begin{aligned} (k+1)T_w V_1(k+1) &= -\left(K_w W(k) + K_p P_e(k) + K_v V_t(k) + V_1(k)\right) \\ V_s(k) &= K_w W(k) + K_p P_e(k) + K_v V_t(k) + V_1(k) \end{aligned} \tag{12}$$

E. Synchronous Machine Model

A detailed 6th order synchronous machine model is given in (13)-(16) including a coordinate transform at the terminal bus for the network interface under the constant impedance load assumption [3], [12].

$$\begin{aligned} T'_{q0}\dot{e}'_d &= -\frac{x_q - x''_q}{x'_q - x''_q}e'_d + \frac{x_q - x'_q}{x'_q - x''_q}e''_d \\ T'_{d0}\dot{e}'_q &= -\frac{x_d - x''_d}{x'_d - x''_d}e'_q + \frac{x_d - x'_d}{x'_d - x''_d}e''_q + e_{fd} \\ T''_{q0}\dot{e}''_d &= e'_d - e''_d + \left(x'_q - x''_q\right)i_q \\ T''_{d0}\dot{e}''_q &= e'_q - e''_q - \left(x'_d - x''_d\right)i_d \\ \dot{\delta} &= \omega_s s_m \\ 2H\dot{s}_m &= p_m - p_e - Ds_m \end{aligned} \tag{13}$$

$$p_e = v_d i_d + v_q i_q$$

$$\begin{bmatrix} i_d \\ i_q \end{bmatrix} = \begin{bmatrix} r_a & -x''_q \\ x''_d & r_a \end{bmatrix}^{-1} \left(\begin{bmatrix} e''_d \\ e''_q \end{bmatrix} - \begin{bmatrix} v_d \\ v_q \end{bmatrix} \right) \tag{14}$$

$$i = \mathbf{Y_r} v \tag{15}$$

$$\begin{bmatrix} i_x \\ i_y \end{bmatrix} = \mathbf{R}\begin{bmatrix} i_d \\ i_q \end{bmatrix}, \quad \begin{bmatrix} v_x \\ v_y \end{bmatrix} = \mathbf{R}\begin{bmatrix} v_d \\ v_q \end{bmatrix}, \quad \text{where } \mathbf{R} = \begin{bmatrix} sin\delta & cos\delta \\ -cos\delta & sin\delta \end{bmatrix} \tag{16}$$

State variables δ, ω, e'_q, e'_d, e''_q and e''_d are respectively the rotor angle, rotor speed, q-axis and d-axis transient voltages and sub-transient voltages; p_e, i_d and i_q are the electrical power and d-axis and q-axis stator currents; v_d and v_q are the d-axis and q-axis terminal voltages; i_x and i_y are the x-axis and y-axis terminal currents; v_x and v_y are the x-axis and y-axis terminal voltages respectively; p_m is the mechanical power; e_{fd} is field voltage; H is the inertia and D is the damping constant; T'_{d0}, T'_{q0}, T''_{d0} and T''_{q0} are the open circuit transient time constants and sub-transient time constants in d-axis and q-axis; x_d, x_q, x'_d, x'_q, x''_d and x''_q are the d-axis and q-axis synchronous reactances, transient reactances and transient reactances; $\omega_s = 2\pi \times 60$ is the nominal frequency and $\mathbf{Y_r}$ is the reduced network admittance matrix.

The DTs of (13)-(16) are given in (17)-(20), where $\Phi(m)$ and $\Psi(m)$ denote the DTs of $\sin\delta$ and $\cos\delta$ obtained by Propositions 2.

$$\begin{aligned}
&(k+1)T'_{q0}E'_d(k+1) = -\frac{x_q - x''_q}{x'_q - x''_q}E'_d(k) + \frac{x_q - x'_q}{x'_q - x''_q}E''_d(k)\\
&(k+1)T'_{d0}E'_q(k+1) = -\frac{x_d - x''_d}{x'_d - x''_d}E'_d(k) + \frac{x_d - x'_d}{x'_d - x''_d}E''_q(k) + E_{fd}(k)\\
&(k+1)T''_{q0}E''_d(k+1) = E'_d(k) - E''_d(k) + (x'_q - x''_q)I_q(k)\\
&(k+1)T''_{d0}E''_q(k+1) = E'_q(k) - E''_q(k) - (x'_d - x''_d)I_d(k)\\
&(k+1)\Delta(k+1) = \omega_s S_m(k)\\
&2(k+1)HS_m(k+1) = P_m(k) - P_e(k) - DS_m(k)
\end{aligned} \tag{17}$$

$$\begin{bmatrix} I_d(k) \\ I_q(k) \end{bmatrix} = \begin{bmatrix} r_a & -x''_q \\ x''_d & r_a \end{bmatrix}^{-1} \left(\begin{bmatrix} E''_d(k) \\ E''_q(k) \end{bmatrix} - \begin{bmatrix} V_d(k) \\ V_q(k) \end{bmatrix} \right) \tag{18}$$

$$P_e(k) = \sum_{m=0}^{k} \left[V_d(m) I_d(k-m) + V_q(m) I_q(k-m) \right]$$

$$I(k) = Y_r V(k) \tag{19}$$

$$\begin{aligned}
\begin{bmatrix} I_x(k) \\ I_y(k) \end{bmatrix} &= \sum_{m=0}^{k} \begin{bmatrix} \Phi(m) & \Psi(m) \\ -\Psi(m) & \Phi(m) \end{bmatrix} \begin{bmatrix} I_d(m-k) \\ I_q(m-k) \end{bmatrix}\\
\begin{bmatrix} V_x(k) \\ V_y(k) \end{bmatrix} &= \sum_{m=0}^{k} \begin{bmatrix} \Phi(m) & \Psi(m) \\ -\Psi(m) & \Phi(m) \end{bmatrix} \begin{bmatrix} V_d(m-k) \\ V_q(m-k) \end{bmatrix}
\end{aligned} \tag{20}$$

F. IEEE Type I Exciter Model

The IEEE Type I exciter model [3], [13] is given in (21)-(23), where e_{fd}, v_f, v_{ts}, v_r are the field voltage, feedback voltage, sensed terminal voltage and regulator voltage; T_e, T_f, T_r, T_a are exciter time constant, feedback time constant, filter time constant and regulator time constant; K_e, K_f, K_a are exciter constants related to self-excited field, feedback gain and regulator gain; s_e is the exciter saturation function which is a nonlinear exponential function determined by the two constants a_e and b_e; v_t is the bus voltage which is a nonlinear square root function; v_{rmax}, v_{rmin} are the maximum and minimum voltage regulator outputs.

$$\begin{aligned}
T_e \dot{e}_{fd} &= v_r - s_e e_{fd} - K_e e_{fd}\\
T_f \dot{v}_f &= -v_f + K_f \dot{e}_{fd}\\
T_r \dot{v}_{ts} &= -v_{ts} + v_t\\
T_a \dot{v}_r &= \begin{cases} -v_r + K_a(v_{ref} + v_s - v_{ts} - v_f), \\ \quad if\, v_{rmin} < v_r < v_{rmax} \\ 0, if\,(v_r = v_{rmax}, \dot{v}_r > 0), OR \\ \quad (v_r = v_{rmin}, \dot{v}_r < 0) \end{cases}
\end{aligned} \tag{21}$$

$$s_e = a_e e^{b_e e_{fd}} \tag{22}$$

$$v_t = \sqrt{v_x^2 + v_y^2} \tag{23}$$

The DTs of (21) is given in (24). Since the DT can handle the discrete events in (21) by deriving the DT for both expressions as shown in the last two equations in (23), they can be switched in the simulation as the traditional method does.

$$\begin{aligned}
&(k+1)T_e E_{fd}(k+1) = V_r(k) - K_e E_{fd}(k) - \sum_{m=0}^{k} S_e(m) E_{fd}(k-m)\\
&(k+1)T_f V_f(k+1) = -V_f(k) + (k+1)K_f E_{fd}(k+1)\\
&(k+1)T_r V_{ts}(k+1) = -V_{ts}(k) + V_t(k)\\
&(k+1)T_a V_r(k+1) = -V_r(k+1)\\
&\qquad + K_a(V_{ref}\delta(k) + V_s(k) - V_{ts}(k) - V_f(k))\\
&(k+1)T_a V_r(k+1) = 0
\end{aligned} \tag{24}$$

However, both (22) and (23) are composite nonlinear functions without existing transform rules. To obtain their DTs, Propositions 3 and 4 proved previously for the composite exponential function and composite square root function are applied. From proposition 3, the DT of the saturation function is given in (25).

$$S_e(k) = a_e \frac{1}{k} \sum_{m=0}^{k-1} (k-m) S_e(m) E_{fd}(k-m) \tag{25}$$

From proposition 4, the DT of terminal voltage is given in (26) -(27), where $u = v_t^2 = v_x^2 + v_y^2$, and $U(k)$ is its DT.

$$U(k+1) = \sum_{m=0}^{k} V_X(m) V_X(k-m) + \sum_{m=0}^{k} V_Y(m) V_Y(k-m) \tag{26}$$

$$V_t(k+1) = \frac{1}{2U(0)} V_t(k) - \frac{1}{2U(0)} \sum_{m=1}^{k-1} U(m) U(k-m) \tag{27}$$

IV. Proposed Scheme for Dynamic Simulation

This section proposes a DT-based scheme for dynamic simulation using the DTs derived above for power system models and then illustrates the scheme using a single-machine-infinite-bus (SMIB) system.

A. DT-based Solution Scheme

The variables of power system model in this paper are given in (28), which satisfy (7), (9), (11), (13)-(16) and (21)-(23).

$$\begin{aligned}
x(t) &= \left[p_{sv}, p_m, v_s, e'_d, e'_q, e''_d, e''_q, \delta, s_m, e_{fd}, v_f, v_r, v_{ts} \right]\\
y(t) &= \left[i_d, i_q, p_e, i_x, i_y, v_d, v_q, v_x, v_y, s_e, v_t \right]
\end{aligned} \tag{28}$$

In the proposed dynamic simulation scheme, these variables are approximated by the K^{th} order power series. After obtaining the coefficients, the trajectory can be displayed by evaluating (29). Thus, the key is to calculate the coefficients $X(k), Y(k), k = 0,1,2\ldots K$ defined by (30).

$$\begin{aligned}
x(t) &= X(0) + X(1)t + X(2)t^2 + \ldots X(K)t^K\\
y(t) &= Y(0) + Y(1)t + Y(2)t^2 + \ldots Y(K)t^K
\end{aligned} \tag{29}$$

$$\begin{aligned}
X(k) &= \left[P_{sv}, P_m, V_s, E'_d, E'_q, E''_d, E''_q, \Delta, S_m, E_{fd}, V_f, V_r, V_{ts} \right]\\
Y(k) &= \left[I_d, I_q, P_e, I_x, I_y, V_d, V_q, V_x, V_y, S_e, V_t \right]
\end{aligned} \tag{30}$$

At each simulation step, $\{X(0),\ Y(0)\}$ are known and $\{X(k),\ Y(k),\ k = 1,2,\ldots K\}$ are to be solved. Algorithm 1 is designed to calculate the $(k+1)^{\text{th}}$ order coefficients from the coefficients of orders $0,1,\ldots k$. The algorithm is executed K-1 times to obtain all the coefficients starting from $\{X(0),\ Y(0)\}$. Since the operations of DT are purely linear, the calculation process is explicit. For example, the coefficients

$P_{sv}(k+1)$ explicitly depend on the lower order coefficients as shown in (8).

Algorithm 1

Input: $X(0:k), Y(0:k)$

Output: $X(0:k+1), Y(0:k+1)$

Steps:

1. Calculate $P_{sv}(k+1)$ from (8).
2. Calculate $P_m(k+\ )$ from (10).
3. Calculate $E_d'(k+1), E_q'(k+1), E_d''(k+1), E_q''(k+1), \Delta(k+1), S_m(k+1)$ from (17).
4. Calculate $I_d(k), I_q(k), P_e(k)$ from (18).
5. Calculate $V_x(k), V_y(k)$ from (19).
6. Calculate $\Phi(k), \Psi(k)$ from (3).
7. Calculate $V_d(k), V_q(k), I_x(k), I_y(k)$ from (20).
8. Calculate $S_e(k), V_t(k)$ from (25)-(27).
9. Calculate $E_{fd}(k+1), V_r(k+1), V_f(k+1), V_{ts}(k+1)$ from (24).
10. Calculate $V_s(k+1)$ from (12).

The DT-based simulation scheme is illustrated below using an SMIB system [1], [3] given in (31) with parameters H=3 s, D=3 p. u., $\omega_s = 2\pi \times 60$ rad/s, P_{max}=1.7 p.u., P_m=0.44 p.u. and the initial state $\delta(0) = 0.26$ rad and $\omega(0) = 0.002$ p.u.

$$\begin{cases} \dot{\delta} = \omega_s \omega \\ \dot{\omega} = \dfrac{1}{2H}\left(P_m - P_{\max}\sin\delta - D\omega\right) \end{cases} \tag{31}$$

To obtain the trajectories of rotor angle and rotor speed, the first step is to apply DT to (31). Similar to the steps described in Section III, its DT is given in (32)-(33):

$$(k+1)\Delta(k+1) = \omega_s W(k) \tag{32}$$

$$2H(k+1)W(k+1) = P_m \varrho(k) - P_{\max}\Phi(k) - DW(k) \tag{33}$$

With the values of parameters plugged in, the recursive formula to calculate the coefficients becomes

$$\begin{aligned} \Delta(k+1) &= \frac{377}{k+1}W(k) \\ W(k+1) &= \frac{1}{k+1}\left[0.073\varrho(k) - 0.283\Phi(k) - 0.5W(k)\right] \end{aligned} \tag{34}$$

The coefficients $\Delta(0), W(0), \Phi(0), \Psi(0)$, are obtained in (35) using Proposition 1-a.

$$\begin{aligned} \Delta(0) &= \delta(0) = 0.26 \\ W(0) &= w(0) = 2\times 10^{-3} \\ \Phi(0) &= \sin(\delta(0)) = 0.2571 \\ \Psi(0) &= \cos(\delta(0)) = 0.9664 \end{aligned} \tag{35}$$

The values of $\Delta(k), W(k)$ for arbitrary k can be calculated starting from (35). For example, the coefficients with k=1 are calculated in (36) with $\varrho(0) = 1$.

$$\begin{aligned} \Delta(1) &= 377W(0) = 0.754 \\ W(1) &= 0.073 - 0.283\Phi(0) - 0.5W(0) = -7.6\times 10^{-4} \\ \Phi(1) &= \Psi(0)\Delta(1) = 0.7287 \\ \Psi(1) &= -\Phi(0)\Delta(1) = -0.1938 \end{aligned} \tag{36}$$

Such a recursive process continues until k reaches a desired order K. The rotor angle and rotor speed expressions for K=3 are approximated by

$$\begin{aligned} \delta(t) &= \Delta(0) + \Delta(1)t + \Delta(2)t^2 + \Delta(3)t^3 \\ w(t) &= W(0) + W(1)t + W(2)t^2 + W(3)t^3 \end{aligned} \tag{37}$$

B. Remarks

In recent literature, other methods have been applied to obtain an approximate solution of a nonlinear differential equation in the form of a polynomial function of time, such as the Adomian decomposition method (ADM) [12]-[13] and a Power Series based method (for short, PSM) [14][15]. The approximate solutions of these two methods and the proposed DT method all converge to the true solution in the power series form when the number of terms increases to infinity [13]-[15], [19], [27]-[28]. However, when finite terms are taken, their solutions are not identical term by term. The main reason lies in their different approximation and truncation mechanisms in generating each specific term: the ADM generates each term as a polynomial of time [12][13] composed of monomials of different orders, so the later terms can also change the coefficients of some of low order monomials when terms grow; the other two methods generate each term as a single monomial of time; the PSM needs to transform all analytical nonlinear functions, e.g. sine and cosine functions, first into truncated Taylor series so as to introduce truncation errors, while the DT method directly uses the differential transforms of nonlinear functions instead of their Taylor expansions.

The solutions of all the above methods are accurate within a limited time window, whose length in general increases with the number of terms. However, their different generation mechanisms make the DT be easier to implement in practice with a large number of terms than the ADM and PSM. The ADM and PSM have to explicitly calculate high order derivatives to obtain Adomian polynomials or truncated Taylor series [13]-[15], [27]-[28]. The complexity of high order derivatives increases significantly at a large number of terms. Comparatively, the DT adopts transform rules to avoid computing high order derivatives [19], [24]. Ref. [17] proposes a Pade Approximants based method to transform a polynomial-form solution, which can be from any of these three methods, into a fractional form to further improve its accuracy, and hence can be applied as a post-processing technique together with each of these three methods.

V. Case Study

In this section, the proposed simulation scheme is tested on the IEEE 10-machine 39-bus system and Polish 327-machine 2383-bus system [27]. The accuracy of the DT approach is validated by various disturbances. The numerical stability,

accuracy and time performance are compared with five commonly used numerical methods [1][3][13]: the modified Euler method (ME), 4th order Runge-Kutta method (RK4), Gill's version of Runge-Kutta method (RKG), Trapezoidal method and Gear method. In all subsections, the benchmark result is given by the RK4 method with a very small time step of 0.3ms. Errors of each method are considered its differences from the benchmark result. Simulations are performed in MATLAB R2017a on a computer with i5-7200U CPU.

A. Scanning Various Contingencies

For the 39-bus system, three stability scenarios, i.e., one stable case, one marginally stable case, and one unstable case, are simulated for 20 seconds. The stable case has a three-phase fault at the bus 3 that starts at t=1s and is cleared after 5 cycles by tripping the line 3-4. The marginal stable and unstable cases are created by clearing the fault after 12.935 cycles and 12.940 cycles, respectively. Fig. 1 to Fig. 3 show the trajectories of rotor angles from both the DT and benchmark RK4 methods as well as the rotor angle errors of the DT method. The machine 1 at bus 30 is selected as the reference. The results of the DT method with K=8 and the time step length of 0.05s accurately match the benchmark results for all three scenarios. The maximum errors of all state variables (including rotor angles, rotor speeds, transient and sub-transient voltages in d-axis and q-axis, field voltages, and all other variables) over the entire 20-second simulation period are 1.48×10^{-4} p.u., 1.00×10^{-3} p.u. and 1.30×10^{-3} p.u. for the three scenarios, respectively.

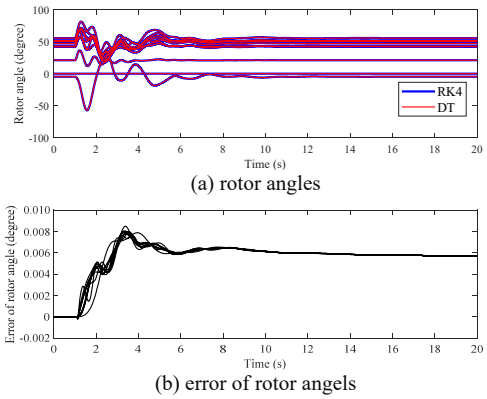

(a) rotor angles

(b) error of rotor angels

Fig. 1. 39-bus system under a stable contingency

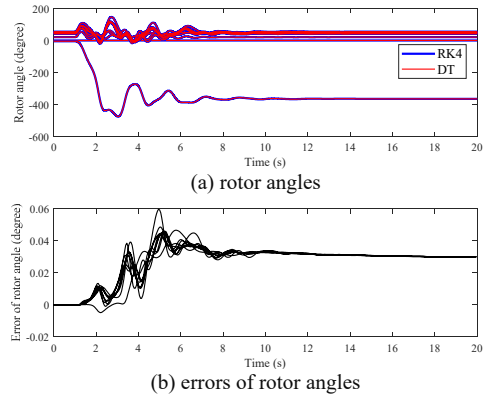

(a) rotor angles

(b) errors of rotor angles

Fig. 2. 39-bus system under a marginal stable contingency.

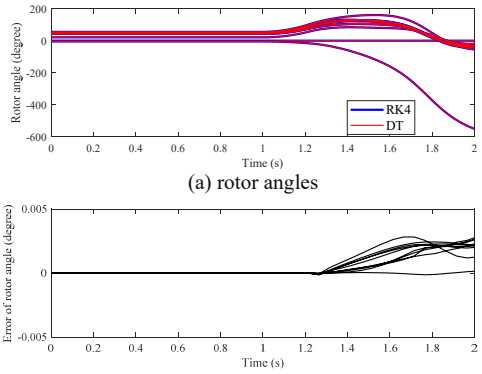

(a) rotor angles

(b) errors of rotor angles

Fig. 3. 39-bus system under marginal unstable contingency.

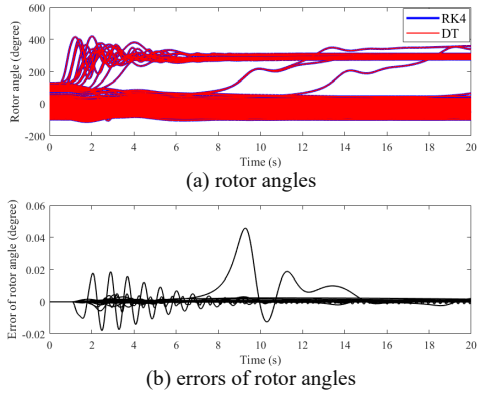

(a) rotor angles

(b) errors of rotor angles

Fig. 4. 2383-bus system under a stable contingency.

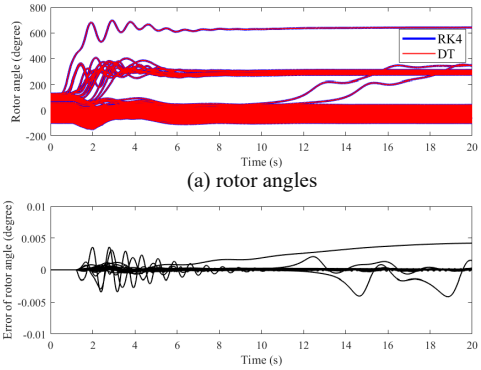

(a) rotor angles

(b) errors of rotor angles

Fig. 5. 2383-bus system under a marginally stable contingency.

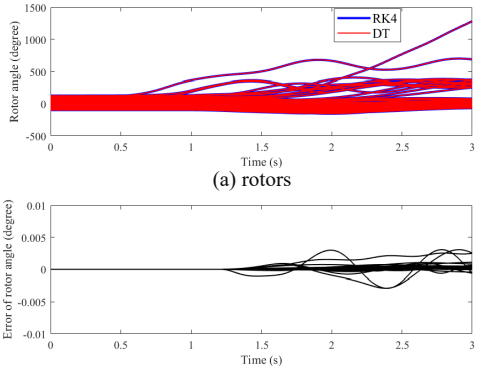

(a) rotors

(b) errors of rotor angles

Fig. 6. 2383-bus system under a marginally unstable contingency.

The same tests are also conducted on the Polish 2383-bus system and the DT method can still assess stability accurately. Fig. 4 to Fig. 6 show the trajectories of rotor angles from both the DT and RK4 methods as well as rotor angle errors of the DT

method using the time step length of 0.016s. The machine 1 at bus 10 is selected as the reference. The maximum errors of all state variables over the entire 20-second simulation period are 5.2×10^{-3} p.u., 3.9×10^{-3} p.u. and 3.8×10^{-3} p.u. for the three scenarios, respectively.

In addition, the impacts of various factors on the simulation of the DT method are studied, including: fault types; fault locations; the modeling of PSS; and the modeling of saliency. Apply these two types of faults to all buses and lines of the 39-bus system: 1) temporary three-phase short-circuit fault lasting for 5 cycles on each bus (totally, 39 faults); 2) permanent three-phase short-circuit line fault near each end of every line that is tripped by opening the line after 5 cycles (totally, 46×2=92 faults). Fig. 7 and Fig. 8 show that the maximum errors are within 1.1×10^{-3} p.u. for any state variables of the system in all cases. Besides, a 830 MW generator trip on bus 38 is simulated and the maximum error is 2.26×10^{-4} p.u..

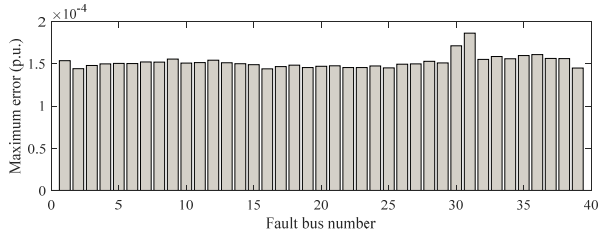

Fig. 7. Accuracy of the DT method when faults occur at all buses.

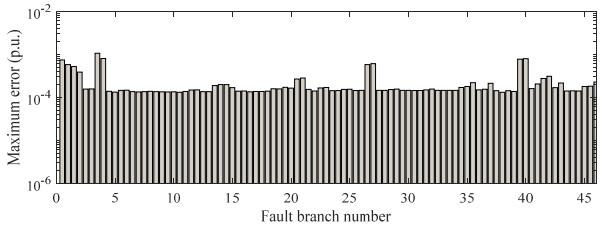

Fig. 8. Accuracy of the DT method when faults occur at all branches.

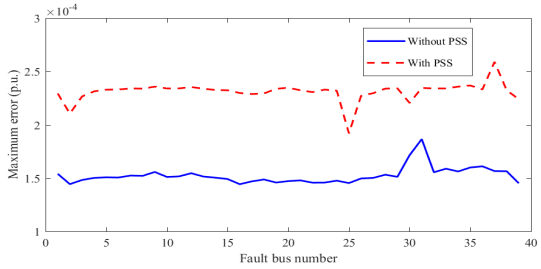

Fig. 9. Accuracy of the DT method with and without PSS.

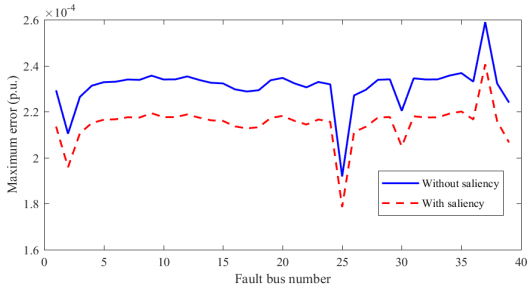

Fig. 10. Accuracy of the DT method with and without saliency.

Also, the impact of the PSS is simulated by many cases. Fig. 9 shows the maximum errors are within 3.0×10^{-4} p.u. and are not affected much by the modeling of PSS. Meanwhile, the impact of the saliency is studied. Fig. 10 shows the maximum errors are within 2.6×10^{-4} p.u. and the modeling of saliency does not introduce additional errors.

B. *Comparison of Numerical Stability*

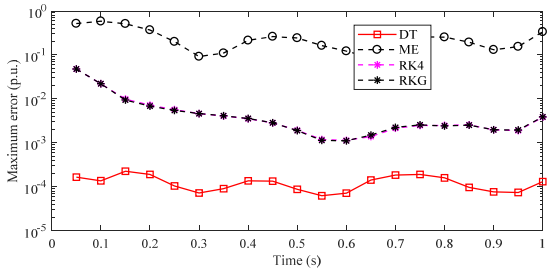

(a) time step = 0.050 s

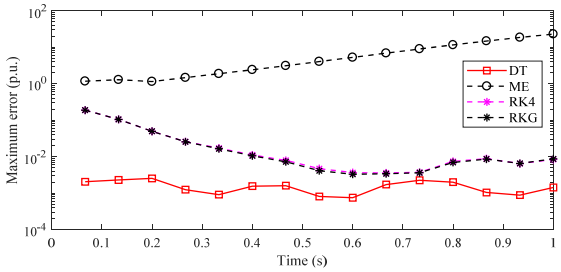

(b) time step =0.067 s

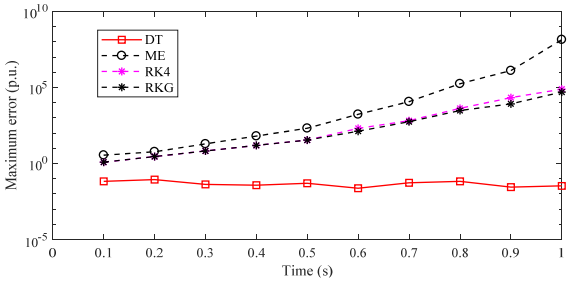

(c) time step = 0.100s

Fig. 11. Error propagation for the three scenarios with different time steps

To study the error propagation and numerical stability, three scenarios are designed for the 39-bus system with three different time step lengths: 0.050s, 0.067s and 0.100s. The simulated disturbance is a three-phase fault at bus 3 cleared after 5 cycles by tripping the branch 3-4. Fig. 11 a)-c) shows the error propagation with the three scenarios where all methods start from the same initial state at t=0s. To take a detailed look at the transient dynamics right after the fault, the figure focuses on the first 1 second. The logarithmic vertical axis is the maximum error of all state variables at the end of each time step. The errors do not propagate much for the four methods when the time step length is 0.050s. Meanwhile, Fig. 11 b) shows the error of the ME method propagates when the time step length is increased to 0.067s and it approaches 10^2 p.u. at t=1.0s, indicating divergence of the ME method. In Fig. 11 c), it shows that the errors of ME, RK4 and RKG methods increase along time steps significantly, indicating the tendency toward numerical instability. Table I summarizes whether the four methods tend to be numerically stable or unstable under three scenarios. All methods work well when the time step length is 0.050s. The ME method has numerical instability issue when the time step length is 0.067s. Only the DT method is

numerically stable under all three scenarios.

TABLE I
COMPARISON OF NUMERICAL STABILITY UNDER THREE SCENARIOS

Time step length (s)	ME	RK4	RKG	DT
0.050	√	√	√	√
0.067	×	√	√	√
0.100	×	×	×	√

Table II summarizes the maximum time step lengths of the four methods to maintain the numerical stability for both the 39-bus system and the 2383-bus system, by extensive simulations with gradually increased time step lengths until numerical instability occurs. The DT approach can maintain numerical stability using much larger time step lengths than the ME, RK4 and RKG methods. But it will diverge when the time step length is larger than 0.125 s for the 39-bus system and 0.017 s for the 2383-bus system. By contrast, the implicit methods such as the Trapezoidal method and the Gear method are very stable, and there is no need to limit their time step lengths from the numerical stability perspective [1]-[3]. These results indicate the numerical stability of the DT approach is better than the ME, RK4, and RKG methods, but weaker than the Trapezoidal method and the Gear method.

TABLE II
COMPARISON OF MAXIMUM TIME STEP LENGTH TO MAINTAIN THE NUMERICAL STABILITY (UNIT: S)

Test systems	ME	RK4	RKG	DT
39-bus system	0.059	0.077	0.077	0.125
2383-bus system	0.007	0.010	0.010	0.017

C. Comparison of Accuracy and Time Performance

For both test systems, Table III shows the time step lengths of the ME, RK4, RKG and DT methods with three desired error tolerances, i.e., the maximum error of all state variables over the entire simulation period is in the magnitude of 10^{-2}, 10^{-3} and 10^{-4} p.u., respectively. For the Trapezoidal and Gear methods, the average time step lengths are shown since they are implemented by MATLAB solvers ode23t and ode15s respectively with variable time step lengths.

For the 39-bus system, the time step lengths of the DT can be increased compared with the ME method to 7.5 times, 23.3 times and 50.0 times while still meeting the requirements of three error tolerances, respectively. Compared with both the RK4 and RKG methods, it is increased to 2.0 times, 2.7 times and 4.5 times. Also, the DT method increases the time step length to 4.5 times and 1.7 times compared to the Trapezoidal and Gear method respectively under the same error tolerance. Similar results are also observed on the 2383-bus system. These results show the DT approach can prolong the time step lengths with the other methods for the same level of error tolerance.

For both test systems, Table IV shows the computation times of the six methods using the time step lengths in Table III. For the 39-bus system, the time costs of the DT method are reduced by 33.3%, 66.4% and 86.8% compared to the ME method under three error tolerances respectively. It is reduced by 15.1%, 17.8%, and 43.2% compared with both the RK4 and RKG methods. Also, the DT reduces the time cost by 61.1% and 11.9% compared to the Trapezoidal and Gear methods respectively under the same error tolerances. Similar results are also observed on the 2383-bus system. These results show the DT approach can reduce computation time compared with the other methods for the same level of error tolerance.

TABLE III
COMPARISON OF TIME STEP LENGTH UNDER DIFFERENT ERROR TOLERANCES (UNIT: S)

Test systems	Error (p.u.)	ME	RK4	RKG	DT	Trapezoidal	Gear
39-bus system	10^{-2}	0.012	0.045	0.045	0.090	0.020	--
	10^{-3}	0.003	0.026	0.026	0.070	--	0.041
	10^{-4}	0.001	0.011	0.011	0.050	--	--
2383-bus system	10^{-2}	0.003	0.010	0.010	0.017	0.004	--
	10^{-3}	0.001	0.007	0.007	0.016	--	0.009
	10^{-4}	0.0005	0.004	0.004	0.012	--	--

TABLE IV
COMPARISON OF COMPUTATION TIME UNDER DIFFERENT ERROR TOLERANCES (UNIT: S)

Test systems	Error (p.u.)	ME	RK4	RKG	DT	Trapezoidal	Gear
39-bus system	10^{-2}	0.42	0.33	0.33	0.28	0.72	--
	10^{-3}	1.10	0.45	0.46	0.37	--	0.42
	10^{-4}	3.71	0.86	0.87	0.49	--	--
2383-bus system	10^{-2}	4.67	3.33	3.29	3.02	1320	--
	10^{-3}	14.10	4.04	4.06	3.67	--	376
	10^{-4}	42.67	8.34	8.29	5.10	--	--

VI. CONCLUSION AND FUTURE WORK

This paper has proposed a DT-based approach for dynamic simulation of multi-machine power systems. This paper derived the DTs for detailed power system models. Then, the simulation scheme using the derived DTs was tested on two test systems. The results show that the approach significantly increases the time step length by using more power series terms to approximate the solution so as to speed up simulation while keeping a comparable accuracy with traditional numerical integration. Therefore, the approach is of great potential for fast power system simulation.

Electricity utilities usually model a power system by a set of nonlinear differential algebraic equations (DAEs) for transient stability studies. In this paper, impedance loads for each simulated system are assumed so as to reduce the original DAE model into a DE model by including loads into a reduced admittance matrix. The simulation results from such a DE model are different from simulation results of a DAE model if more complex loads exist. This paper has focused on a proof of concept study on the DT method for simulating a large-scale

system and several important aspects of handling DEs for power system simulation including transformation rules specifically for nonlinear power system models, practical DE models of generators and their controllers and detailed comparisons of the DT method with other numerical methods. Extending the proposed approach to solve power system DAEs will be our next focus of research.

APPENDIX

Proof of Proposition 3: From $\dot{y}_1 = y_1\dot{x}$, there is

$$(k+1)Y_1(k+1) = \sum_{m=0}^{k} Y_1(m)\cdot(k+1-m)X(k+1-m)$$

For convenience, it can be written as:

$$Y_1(k+1) = \frac{1}{(k+1)}\sum_{m=0}^{k}(k+1-m)Y_1(m)X(k+1-m)$$

Replacing *k* by *k-1* will lead to (4). ■

Proof of Proposition 4: From $y_2^2 = x$, there is

$$\sum_{m=0}^{k} Y_2(m)Y_2(k-m) = X(k)$$

$$2Y_2(0)Y_2(k) + \sum_{m=1}^{k-1} Y_2(m)Y_2(k-m) = X(k)$$

Then, it is easy to obtain (5). ■

Proof of Proposition 5: Observe that $x = zy$, we have

$$\sum_{m=0}^{k} Z(m)Y(k-m) = X(k)$$

$$Y(0)Z(k) + \sum_{m=0}^{k-1} Z(m)Y(k-m) = X(k)$$

Then, it is easy to obtain (6). ■

REFERENCES

[1] P. Kundur, N. J. Balu, M. G. Lauby, *Power system stability and control*. McGraw-hill New York, 1994.

[2] B. Stott, "Power system dynamic response calculations," *Proc. of the IEEE*, vol. 67, no. 2, pp. 219–241, 1979.

[3] F. Milano, *Power system modelling and scripting*. Springer Science & Business Media, 2010.

[4] S. Zadkhast, J. Jatskevich, E. Vaahedi, "A multi-decomposition approach for accelerated time-domain simulation of transient stability problems," *IEEE Trans. on Power Syst.*, vol. 30, no. 5, pp. 2301-2311, Sep. 2015.

[5] Y. Liu, Q. Jiang, "Two-stage parallel waveform relaxation method for large-scale power system transient stability simulation," *IEEE Trans. on Power Syst.*, vol. 31, no. 1, pp. 153-162, Jan. 2016.

[6] P. Aristidou, S. Lebeau, T. V. Cutsem, "Power system dynamic simulations using a parallel two-level Schur-complement decomposition," *IEEE Trans. on Power Syst.*, vol. 31, no. 5, pp. 3984-3995, Sep. 2016.

[7] G. Gurrala, et al, "Parareal in time for fast power system dynamic simulations," *IEEE Trans. Power Syst.*, vol. 31, no. 3, pp. 1820-1830, Jul. 2015.

[8] N. Duan, et al, "Applying reduced generator models in the coarse solver of parareal in time parallel power system simulation," in Proc. *IEEE PES Innovative Smart Grid Technologies Conference Europe*, 2016, pp. 1-5.

[9] M. A. Tomim, et al, "Parallel transient stability simulation based on multi-area Thévenin equivalents," *IEEE Transactions on Smart Grid,* vol. 8, no. 3, pp. 1366-1377, 2017.

[10] R. Diao, S. Jin, F. Howell, "On parallelizing single dynamic simulation using HPC techniques and APIs of commercial software," *IEEE Trans. on Power Syst.*, vol. 32, no. 3, pp. 2225-2233, May. 2017.

[11] I. Konstantelos, et al, "Implementation of a massively parallel dynamic security assessment platform for large-scale grids," *IEEE Trans. on Smart Grid*, vol. 8, no. 3, pp. 1417-1426, May 2017.

[12] N. Duan, K. Sun, "Power system simulation using the multi-stage Adomian Decomposition Method," *IEEE Trans. on Power Syst.*, vol. 32, no. 1, pp 430-441, Jan. 2017.

[13] G. Gurrala, D. L. Dinesha, A. Dimitrovski, et al, "Large multi-machine power system simulations using multi-Stage Adomian Decomposition," *IEEE Trans. on Power Syst.*, in press.

[14] E. Abreut, B. Wang, K. Sun, "Semi-analytical fault-on trajectory simulation and its application in direct methods," in Proc. *Power and Energy Society General Meeting*, 2017, pp. 1-5.

[15] B. Wang, N. Duan, K. Sun, "A Time-Power Series Based Semi-Analytical Approach for Power System Simulation," *IEEE Trans. Power Syst.*, vol. 34, No. 2, pp. 841-851, March 2019

[16] C. Liu, B. Wang, K. Sun, "Fast power system simulation using semi analytical solutions based on Pade Approximants," in Proc. *Power and Energy Society General Meeting*, 2017, pp. 1-5.

[17] C. Liu, B. Wang, K. Sun, "Fast Power System Dynamic Simulation Using Continued Fractions," *IEEE Access*, vol. 6, No. 1, pp. 62687-62698, 2018

[18] E. Pukhov, G. Georgii, "Differential transforms and circuit theory," *International Journal of Circuit Theory and Applications*, vol. 10, no. 3, pp. 265-276, Jun. 1982.

[19] I. H. A. Hassan, "Application to differential transformation method for solving systems of differential equations," *Applied Mathematical Modelling*, vol. 32, no. 12, pp. 2552-2559, Oct. 2007.

[20] M. Ghafarian, A. Ariaei, "Free vibration analysis of a system of elastically interconnected rotating tapered Timoshenko beams using differential transform method," *International Journal of Mechanical Sciences*, vol. 107, pp. 93-109, 2016.

[21] M. Matinfar, S. R. Bahar, M. Ghasemi, "Solving the Lienard equation by differential transform method," *World Journal of Modelling and Simulation*, vol. 8, no. 2, pp. 142-146, 2012.

[22] L. Xie, C. Zhou, S. Xu, "An effective numerical method to solve a class of nonlinear singular boundary value problems using improved differential transform method," *SpringerPlus*, vol. 5, no. 1, pp. 1066, Jul. 2016.

[23] F. Kenmogne, "Generalizing of differential transform method for solving nonlinear differential equations," *Applied & Computational Mathematics*, vol. 4, no. 1, pp. 1000196, Jan. 2015.

[24] V. S. Erturk, Z. M. Odibat, S. Momani, "The multi-step differential transform method and its application to determine the solutions of non-linear oscillators," *Advances in Applied Mathematics and Mechanics*, vol. 4, no. 4, pp. 422-438, Aug. 2012.

[25] C. W. Berta, H. Zeng, "Analysis of axial vibration of compound bars by differential transformation method," *Journal of Sound and Vibration*, vol. 275, no. 3, pp. 641-647, Aug. 2004.

[26] Z. Odibat, S. Momani, "A generalized differential transform method for linear partial differential equations of fractional order," *Applied Mathematics Letters*, vol. 21, no. 2, pp. 194-199, Feb. 2008.

[27] S. Ghosh, A. Roy, D. Roy, "An adaptation of adomian decomposition for numericanalytic integration of strongly nonlinear and chaotic oscillators," *Comput. Methods Appl. Mech. Eng.*, vol. 196, pp. 1133–1153, 2007.

[28] G. Adomian, "A review of the decomposition method and some recent results for nonlinear equations," *Comput. Math. Appl.*, vol. 21, no. 5, pp. 101–127, 1991.

[29] R. D. Zimmerman, et al, "Matpower: Steady-state operations, planning and analysis tools for power systems research and education," *IEEE Tran. Power Syst.*, vol. 26, no. 1, pp. 12–19, 2011.

Yang Liu (S'17) received the B.S. degree in energy and power engineering from Xi'an Jiaotong University, China, in 2013, and the M.S. degree in power engineering from Tsinghua University, China, in 2016, respectively. He is currently pursuing the Ph.D. degree at the Department of Electrical Engineering and Computer Science, University of Tennessee, Knoxville, USA. His research interests include power system simulation, stability and control.

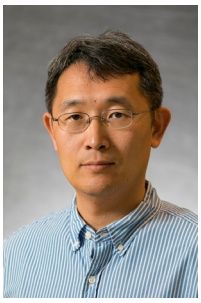

Kai Sun (M'06–SM'13) received the B.S. degree in automation in 1999 and the Ph.D. degree in control science and engineering in 2004 both from Tsinghua University, Beijing, China. He is an associate professor at the Department of EECS, University of Tennessee, Knoxville, USA. He was a project manager in grid operations and planning at the EPRI, Palo Alto, CA from 2007 to 2012. Dr. Sun serves in the editorial boards of IEEE Transactions on Power Systems, IEEE Transactions on Smart Grid, IEEE Access and IET Generation, Transmission and Distribution.

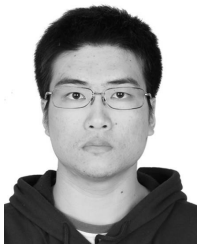

Rui Yao (S'12–M'17) received the B.S. degree (with distinction) in 2011 and Ph.D. degree in 2016 in electrical engineering at Tsinghua University, Beijing, China. He was a postdoctoral research associate at the University of Tennessee, Knoxville during 2016–2018. He is currently a postdoctoral appointee at Argonne National Laboratory.

Bin Wang (S'14) received the B. S. and M.S. degrees from Xi'an Jiaotong University in 2011 and 2013, respectively, and Ph.D. degree from the University of Tennessee, Knoxville, all in Electrical Engineering. He is currently a postdoc researcher in the Department of Electrical and Computer Engineering at Texas A&M University. His research interests include power system dynamics, stability and control.